Determination of size, size distribution and concentration of nanoparticles using ICP-MS in the context of SERS substrates

Julie Horne[a*], Pierre Beckers[a], Kevser Kemik[a], Charlotte De Bleye[a], Pierre-Yves Sacré[b], Nicolas Thelen[c], Philippe Hubert[a], Eric Ziemons[a†], Cédric Hubert[a†*]

[a] *University of Liege (ULiege), CIRM, ViBra-Sante HUB, Laboratory of Pharmaceutical Analytical Chemistry, Department of Pharmacy, Liege, Belgium*

[b] *University of Liege (ULiege), CIRM, Research Support Unit in Chemometrics, Department of Pharmacy, Liege, Belgium*

[c] *University of Liege (ULiege), GIGA-Neurosciences, Cellular and tissular biology, Liege, Belgium*

[*] *Correspondence: julie.horne@uliege.be, chubert@uliege.be*

[†] *These authors contributed equally to this work*

Abstract

Surface enhanced Raman scattering (SERS) is a widely used vibrational spectroscopic technique employing metallic nanostructures to enhance an inherent Raman signal. This study aimed to develop a method for the characterization of SERS substrates in a single analysis by inductively coupled plasma mass spectrometry (ICP-MS) equipped with the single particle module (spICP-MS). For this development, the well-known Lee-Meisel protocol was selected as starting point to synthesize gold nanoparticles (AuNps) and silver nanoparticles (AgNps). A spICP-MS method was successfully developed and gave the mean size, size distribution and concentration of nanoparticles in only one single analysis. Reference techniques were used to confirm these results namely dynamic light scattering, transmission electron microscopy and UV-Visible spectroscopy. Thanks to the ICP-MS characterization, it was observed that AgNps synthesized by chemical reduction presented more variability than the AuNps. The dissolved elements concentration in the suspension was investigated. It appeared that reaction yields were close to 100% for the six syntheses. This analysis may be repeated over time to evaluate the suspension stability and monitor any potential degradation of Nps. To conclude, ICP-MS is a powerful technique to characterize SERS substrates and could be an interesting alternative to other characterization techniques.

Keywords: single particle inductively coupled plasma mass spectrometry (spICP-MS) – metallic nanoparticles (Nps) – SERS substrates – Size characterization

1. Introduction

Surface-enhanced Raman scattering (SERS) is known worldwide as a vibrational technique offering qualitative and quantitative information[1–3]. This technique employs metallic nanoparticles (Nps) which are generally composed of gold (AuNps) or silver (AgNps)[4]. These Nps also called SERS substrates, can enhance the Raman signal of an analyte through the close surface interaction of Nps and the analyte itself[5]. Commercial substrates are still not widely employed for SERS analyses because of their elevated price, their weak Nps concentration and the presence of inadequate additives (often undisclosed) that may generate poor or unreliable signal. That is one of the main reasons why an important number of researchers prefer to synthesize their own substrates, generally in a suspension form[6–8]. However, given that Nps properties directly influence SERS signal intensity, their characterization turns out indispensable[9]. Different analytical techniques are currently available to obtain multiple information about shape, size, and size distribution of nanoparticles such as electronic microscopy, dynamic light scattering (DLS) or UV-Visible spectroscopy to cite a few[10,11]. However, as none of them can provide information on all properties, a combination of these techniques is required to achieve a comprehensive characterization.

This innovative study presents an interesting tool to rapidly characterize SERS substrates using a single technique: the inductively coupled plasma mass spectrometry (ICP-MS). This technique was initially developed to quantify most of the elements of the periodic table with a very high sensitivity, within the ppt range[12]. Analyses are very promptly conducted, and the specificity of the method is guaranteed through the mass spectrometry detector. Briefly, the principle of the ICP-MS comprises the injection of a noble gas (argon) into a nebulizer to transform the liquid sample into an aerosol[12,13]. The aerosol is simultaneously vaporized, atomized and ionized in a plasma of approximately 8000° C[14]. A succession of two cones and four lenses will select the ions of interest and redirect the beam to the quadrupole. The latter

will extract the ions of desired mass to charge (m/z) ratio to finally quantify it by an electron multiplier[12].

ICP-MS has been recently enhanced with an integrated single particle analysis mode (spICP-MS) enabling comprehensive characterization of Nps[15]. Size, size distribution and concentration of Nps can be simultaneously determined in a single analysis. Additionally, ICP-MS can be used to determine the concentration of metallic element in the suspension which provides valuable insight into the completeness of the synthesis or potential degradation of Nps[16–18]. Like many characterization techniques that assess size, spICP-MS assumes that the nanoparticles are spherical which makes this tool particularly suitable for spherical substrates [19,20]. However, ICP-MS can still be used to determine dissolved salts for any type of SERS amplifier. Size determination involves the injection of Nps with the appropriate dilution to get only one particle at a time into the plasma[21–23]. If multiple Nps enter the torch at the same analysis time interval (also called dwell time), they may be detected as a single larger Np leading to biased results. Dwell time is thus a critical parameter for spICP-MS analyses directly influencing the results quality[24,25]. This period of time is generally comprised between 3 and 10 ms[14,24]. However, reducing the dwell time to 0.1 ms can significantly mitigate the impact of the dissolved ions on the obtained results[26]. Such brief dwell times are achievable with the fast data acquisition hardware of ICP-MS. High dissolved ion concentrations can influence the measured size and leads to an overestimation of this latter[27]. On the other hand, Nps that are to small cannot be distinguished from the background noise of dissolved ions[28]. Thus, to obtain accurate spICP-MS results, the sample preparation with the appropriate dilution is crucial.

Another aspect to keep in mind is the fact that the nebulization efficiency (Neb_{eff}) of the calibration material, which was determined in the beginning of the analysis, is considered as identical for the analyzed Nps[29]. In fact, Neb_{eff} represents the amount of sample arriving to the plasma and is generally comprised between 2 and 10 % when using a traditional glass

concentric nebulizer[20]. This value depends on multiple parameters such as the nebulizer gas nature, the gas flow rate and the sample viscosity and has a critical impact on the results[20]. Neb_{eff} may be estimated using a reference material (RM) of a well-known size or concentration[30]. The calculation based on the size is generally recommended because the acquired value is more stable and reliable than the value obtained through the concentration.

In practice, each Np generates a peak while the blank baseline is the direct reflection of the ionic content for a specific element[20]. To be considered, each nanoparticle needs to induce a spike with an intensity significantly different from the background[24]. The peak frequency illustrates the Nps concentration while the size is correlated to their intensity[21,25,28].

The objective of this study was to develop an analytical method to characterize SERS substrates in a single analysis with a simple and rapid sample preparation. By means of spICP-MS, average size, size distribution and concentration of Nps will be determined. Therefore, conventional ICP-MS mode was also used to determine the dissolved ions concentration in complement to the size determination by spICP-MS mode. The developed procedure is applied on freshly synthetized homemade Lee-Meisel SERS substrates of gold and silver[31]. However, this methodology can be extended to substrates obtained through alternative synthesis route as well as to other types of nanoparticles such as copper nanoparticles or silica cores coated with a metallic layer. Transmission electronic microscopy (TEM), DLS and UV-Visible spectroscopy were used as reference techniques and compared to ICP-MS results.

2. Materials and Methods

2.1 Chemicals and reagents

Silver nitrate (analytical grade), potassium chloride (analysis grade) silver solution 1000 µg/mL and gold solution 1000 µg/mL (ICP-MS grade) were purchased from VWR (Pennsylvania, USA) while trisodium citrate (analytical grade) was obtained from Acros Organics (Geel,

Belgium). Crystal violet (analysis grade) was purchased from TCI Europe N.V. (Zwijndrecht, Belgium). Chlorauric acid (analytical grade), gold nanoparticles of 60 nm and silver nanoparticles of 60 and 80 nm were provided from Sigma-Aldrich (Saint-Louis, Missouri, USA). The suspension of gold nanoparticles of 30 nm came from LGC (Teddington, UK). These suspensions were purchased based on the suspension media, namely suspended in a citrate buffer to avoid variations of Neb_{eff} between the samples and the calibration. Iridium solution 1000 µg/mL and rhodium solution 1000 µg/mL (ICP-MS grade) were acquired from Merck (Darmstadt, Germany). A tuning solution was used to calibrate the ICP-MS system, containing several elements (Li, Co, Mg, Y, Ce, Tl) at the concentration of 1 ng/mL (Agilent Technologies, Santa Clara, California, USA). All solutions and dilutions (except for ICP-MS measurements) were made using MilliQ water (18.2 MΩ.cm, Milli-Q Plus 185, Millipore, Burlington, USA). For ICP-MS analyses, dilutions were made using a solution of diluted nitric acid. The nitric acid 67-69 % (trace metal grade) was bought from Fischer Scientific (Hampton, New Hampshire, USA).

2.2 Nanoparticles synthesis

Gold and silver nanoparticles were prepared by chemical reduction according to the Lee and Meisel protocol[31]. Synthesis parameters for each protocol of Nps are reported in the Table 1. Briefly, a metallic solution was introduced into a tripleneck round-bottom flask and was magnetically homogenized and heated by a Drysyn oil heating bath (Asynt, England). Trisodium citrate (0.04 M) was added to the boiling solution through a free neck of the flask by a dosing device (Dosimat, Metrohm AG, Switzerland). After one hour of reaction, the heating was stopped, and the suspension was left to cool down at ambient temperature. All the syntheses were protected from light to avoid potential degradation and the resulting suspension was stored at a temperature of 4° C, in the dark. Three independent syntheses of AuNps and AgNps were prepared following this procedure.

Table 1. Synthesis conditions for silver (AgNps) and gold nanoparticles (AuNps)

	AgNps	AuNps
Reactant	$AgNO_3$	$HAuCl_4$
Reactant weight/ mg	45	48
Volume of reactant solution/ mL	250.0	100.0
Reaction temperature/ °C	180	150
Citrate solution volume added/ mL	5	10
Citrate addition rate/ mL/min	5	5

2.3 SERS analyses

SERS spectra were recorded using a handled Raman analyzer (TruScan™ RM with the TruTools™ package, Thermo Fisher Scientific, Waltham, MA, USA). The laser wavelength was 785 nm with a spectral resolution comprised between 8 and 10.5 cm^{-1} and a spectral range from 250 to 2875 cm^{-1}. For analyses, 3 accumulations of 500 ms were taken at a laser power of 75 mW. Samples were prepared by mixing with a vortex (Reax top, Heidolph, Schwabach, Germany), 400 µL of nanoparticles suspension with 400 µL of crystal violet 1 x 10^{-6} M. Finally, 100 µL of aggregating agent (potassium chloride 0.1 M) were added to the suspension and mixed 10 s before the acquisition. Three replicates were prepared for each kind of substrate. SERS spectra were preprocessed with MatLab® R2020b (The MathWorks, Natick, MA, USA) and the PLS_Toolbox 8.9.2 (Eigenvector Research, Inc., Wenatchee, WA, USA). The preprocessing was a correction of the baseline (Whittaker filter with λ: 30 000 and p: 0.01).

2.4 Characterization methods & instrumentation

2.4.1 ICP-MS analyses for dissolved element determination

ICP-MS analyses were acquired by an ICP-MS 7800 (Agilent Technologies, Santa Clara, California, USA) with a torch of 2.5 mm of internal diameter, nickel cones and 1.0 L/min for the nebulizer gas flow rate. The software is MassHunter 5.2 (Agilent Technologies, Santa Clara, California, USA). At the startup of the plasma and before the analysis, an autotune is realized to optimize the system parameters and minimize the potential interferences (oxide ratios and

doubly charged ions) with the tuning solution. During this autotune, the pulse/analogue factor is also optimized. The general chapter of European Pharmacopeia (Ph. Eur.) for ICP-MS was respected considering a limit test for all the analyses[32]. These were conducted in general purpose plasma mode, the acquisition mode was set on spectrum with 1 point of peak pattern, with 5 replicates and 100 sweeps per replicate. The acquisition time was fixed at 0.1 s for internal standards and 1.0 s for gold and silver. Rinse and diluent solutions were composed of nitric acid at a concentration of 1.92% (w/v). Calibration curve contained a blank and multiple solutions from 5 to 40 ng/mL for silver and from 5 to 30 ng/mL for gold. A quality control (QC) was prepared at 15 ng/mL. Internal standard was a 25 ng/mL solution composed of iridium (Ir) and rhodium (Rh) was injected all along the analysis through its own tubing. Three independent replicates were prepared and analyzed for each Nps suspensions synthesis. Gold and silver were analyzed separately for practical reasons. Nps were removed from the samples by 3 consecutive centrifugations (11 000 rpm during 15 min). Indeed, to ensure that only dissolved metallic ions are analyzed, Nps need to be physically eliminated to avoid their dissolution by nitric acid. The final supernatant was injected into the ICP-MS system.

2.4.2 spICP-MS analyses

The employed equipment was an ICP-MS 7800 (Agilent Technologies, Santa Clara, California, USA) coupled to the MassHunter 5.2 software (Agilent Technologies, Santa Clara, California, USA). The nebulizer gas flow rate was set on 0.80 L/min while the sample inlet flow was 0.346 mL/min depending on the internal diameter of the torch (1.5 mm) and the diameter of the sample tubing, respectively. Thanks to the fast data acquisition hardware, dwell time was fixed on 0.1 ms with an acquisition time of 60 s per injection. Given that Nps are composed of only one constituent, the mass fraction was set on 1 for all the suspensions. Gold density was fixed on 19.32 g/cm³ and the 197 isotope was monitored. For silver, the density was set on 10.50 g/cm³ with the 107 isotope. Rinse solution as well as the blank solution were composed of

MilliQ water. Ionic solutions of silver and gold were prepared at 1 ng/mL. Suspensions were sonicated 2 minutes before being diluted with water to avoid a Nps aggregation. Each synthesis was injected in a separate sequence with three independent replicates. Commercial AgNps of 60 nm and AuNps of 32.7 nm (based on the analysis certificate) were used as reference material (RM) and the quality control (QC) consisted of commercial AgNps of 80 nm and AuNps of 60 nm for silver and gold analyses respectively. Dilution factors for all suspensions are presented in Table 2.

Table 2. Dilution factors for all suspensions analyzed by spICP-MS

	AgNps	AuNps
Reference material (RM)	1 000 000	1 250 000
Samples	1 000 000	13 333 333
Quality control (QC)	200 000	1 000 000

2.4.3 Reference methods for Nps characterization

To confirm the accuracy of spICP-MS results, they were compared with those obtained with reference methods. First, transmission electron microscopy (TEM) images were generated with a Jeol JEM-1400 TEM (Jeol, Tokyo, Japan) at 80 kV with a maximum magnification set on 60 000. A drop of 11 µL of Nps suspension was deposited and left to dry on a 200 mesh copper coated carbon grid (Jeol, Tokyo, Japan) prior to the TEM analyses. EMSIS iTEM Software (Münster, Germany) was then used to measure the average size of AgNps and AuNps based on the measurement of the diameter of 100 individual Nps.

Second, dynamic light scattering (Malvern Panalytical ZetaSizer Nano ZS DLS, Malvern Panalytical, Malvern, United Kingdom) was used with a 632.8 nm wavelength laser to measure the mean size and the size dispersion of synthesized Nps. The zeta potential, reflecting the suspension stability, was also determined by an electrophoretic light scattering (ELS) equipment (Malvern Panalytical, Malvern, United Kingdom). For these analyses, suspensions

were diluted 10 times and sonicated before being added into a specific cuvette (Malvern Panalytical, Malvern, United Kingdom). Size dispersion was estimated by the width of the deconvoluted peak according to a logistic shape using the *ipf* function (version 12)[33] running in MATLAB® R2020b (The MathWorks, Natick, MA, USA).

Finally, UV-Visible spectra (Lambda 40, PerkinElmer, Waltham, Massachusetts, USA) were recorded from 300 to 800 nm. Ten-times diluted suspensions were sonicated prior to the UV-Visible measurement.

3. Results and discussion

3.1 SERS acquisitions

SERS measurements were conducted to confirm the suitability of the synthesized AgNps and AuNps as SERS substrates and to demonstrate that the characterization method developed in this study is appropriate for the analysis of SERS substrates. Figure 1a presents a SERS spectrum of crystal violet obtained using gold nanoparticles while Figure 1b shows the SERS spectrum acquired with silver nanoparticles. As expected, the synthesized AuNps and AgNps generated an intense SERS response validating their use in the development of the spICP-MS characterization method.

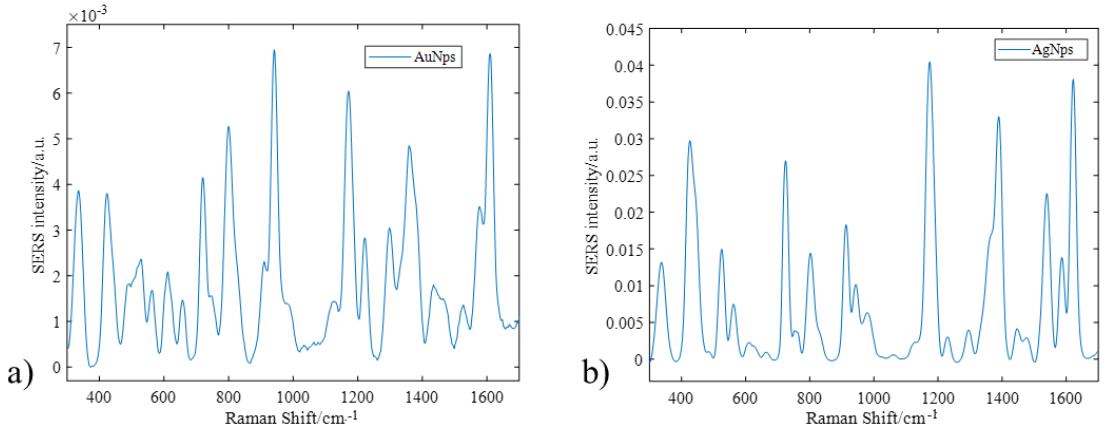

Figure 1. SERS spectra of crystal violet (1 x 10^{-6} M) obtained with gold nanoparticles (a) or silver nanoparticles (b) which were homemade synthesized.

3.2 ICP-MS analyses for dissolved element determination

While single particle mode is capable to quantify dissolved element, its ability to distinguish Nps from ionic content is not perfectly achieved through that module[28]. Moreover, the sample dilution applied for spICP-MS analyses leading to very low element concentrations is not compatible with the single particle accuracy. Conventional ICP-MS was then used to determine the concentration of dissolved metallic ions present in the suspensions. The determination of this concentration brings relevant information since it indicates the reaction yield and can also serve to monitor the Nps stability over time. For instance, an increase in the dissolved metal ions concentration may suggest Nps degradation[18]. Despite its significance, this point is often overlooked in nanoparticle characterization studies.

According to the ICP-MS principle, a calibration curve was plotted for both gold and silver elements. The correlation coefficients are higher than 0.99 (Ph. Eur. guideline) with values of 1.00 for both elements. Detection limit was also estimated during each analysis taking into account that several factors such as the equipment status, the sample matrix or the diluent can influence this limit[34]. Detection limit was evaluated at 11 and 7 ppt for gold and silver, respectively. For the quality control and the internal standard, a recovery range from 80 to 120% was required and all these criteria are conform. Furthermore, relative standard deviation (RSD) for all the injections (except for blanks) did not exceed the tolerated 5% according to the Ph. Eur. guidelines. Concerning the samples, as illustrated in Table 3, yields of reaction are very close to 100%, implying that all silver nitrate and chlorauric acid in the suspensions were consumed by the trisodium citrate to form Nps. These results were expected given that trisodium citrate was added in excess to the reaction. Indeed, citrate is commonly used to reduce metallic salt but also to stabilize the suspension. Dilutions and weightings were considered to calculate the reaction yields based on the ICP-MS concentration.

Fig. S1 resumes the sequential steps for conducting an ICP-MS analysis.

Table 3. ICP-MS results for AgNps and AuNps suspensions

AgNps		ICP-MS concentration/ ng/mL	Reaction yield/ %	AuNps		ICP-MS concentration/ ng/mL	Reaction yield/ %
Synthesis 1	Replicate 1	18.28	99.98	Synthesis 1	Replicate 1	9.90	99.99
	Replicate 2	12.13	99.99		Replicate 2	8.97	99.99
	Replicate 3	29.45	99.97		Replicate 3	8.84	99.99
Synthesis 2	Replicate 1	15.89	99.99	Synthesis 2	Replicate 1	27.70	99.99
	Replicate 2	19.86	99.98		Replicate 2	28.41	99.99
	Replicate 3	23.39	99.98		Replicate 3	24.05	99.99
Synthesis 3	Replicate 1	38.37	99.97	Synthesis 3	Replicate 1	11.23	99.99
	Replicate 2	40.44	99.97		Replicate 2	12.03	99.99
	Replicate 3	41.08	99.97		Replicate 3	11.87	99.99

3.3 spICP-MS analyses

During spICP-MS analyses, several parameters were checked to validate the sequence and to ensure the reliability of the obtained results. Among them, the most significant one is the nebulization efficiency (Neb_{eff}) that must be comprised between 2 and 10 %. This percentage represents the fraction reaching the plasma for the measurements and is determined by the equipment, based on the RM size. The second focus point is the number of detected Nps indicating the possible presence of aggregates or an inappropriate dilution of the samples. It is recommended to measure from 500 to 2000 Nps per injection on average[35]. Although the RM nature used for the calibration can be different from the nature of the analyzed Nps, the single particle mode required the same element for all the samples consideration. Consequently, each synthesis was analyzed in a separate sequence. In practice, a specific sequence for each synthesis was created with three replicates per synthesis. Samples containing Nps were prepared daily to avoid aggregation or dissolution[20,30]. RM should be analyzed rapidly after opening because Nps will gradually dissolve, enhancing the ionic content and decreasing the measured size[19]. Fig. S2 summarizes the sequential steps for conducting a spICP-MS analysis.

The Tables 4 and 5 show the Neb_{eff}, the number of particles and the results for each injection for the AuNps and AgNps syntheses. Given that Neb_{eff} falls within the recommended range and that Nps size for RM and QC are consistent with the values stated in the analysis certificates, the results obtained for samples are considered valid.

Table 4. spICP-MS results for AuNps syntheses

AuNps		Neb_{eff}/ %	Particle number	Particle concentration/ x10^7 particles/L	Mean equivalent diameter/ nm
Synthesis 1	RM (32.7 nm)	5.7	1814	9.2	32
	Replicate 1		1324	6.7	26
	Replicate 2		1284	6.5	25
	Replicate 3		1473	7.5	26
	QC (60 nm)		300	1.5	56
Synthesis 2	RM (32.7 nm)	6.0	1975	9.5	32
	Replicate 1		1813	8.7	24
	Replicate 2		1748	8.4	24
	Replicate 3		1805	8.7	24
	QC (60 nm)		289	1.4	58
Synthesis 3	RM (32.7 nm)	5.7	1866	9.4	32
	Replicate 1		1748	8.8	24
	Replicate 2		1593	8.0	24
	Replicate 3		1545	8.1	24
	QC (60 nm)		301	1.5	58

Neb_{eff} = nebulization efficiency, RM = reference material, QC= quality control

Table 5. spICP-MS results for AgNps syntheses

AgNps		Neb_{eff} / %	Particle number	Particle concentration/ $x10^7$ particles/L	Mean equivalent diameter/ nm
Synthesis 1	RM (60 nm)	2.8	282	2.9	58
	Replicate 1		1014	11	63
	Replicate 2		972	10	63
	Replicate 3		1067	11	56
	QC (80 nm)		655	6.8	71
Synthesis 2	RM (60 nm)	2.8	307	3.2	58
	Replicate 1		708	7.4	65
	Replicate 2		730	7.6	65
	Replicate 3		718	7.5	63
	QC(80 nm)		680	7.1	69
Synthesis 3	RM (60 nm)	2.2	295	3.8	58
	Replicate 1		1219	16	48
	Replicate 2		1342	17	47
	Replicate 3		1460	19	46
	QC (80 nm)		600	7.7	67

Neb_{eff} = nebulization efficiency, RM = reference material, QC= quality control

As shown in Tables 4 and 5, the replicates exhibit comparable values to each other in terms of both concentration and Nps sizes. The relative standard deviations (RSD) for the measured sizes of replicates are less than 6.7 % per synthesis. In contrast, batch-to-batch comparison indicates that AuNps tend to be more uniform in size and concentration than AgNps which exhibit more variability between the batches. This observation is coherent with the heterogeneous character of AgNps reported in the literature[36].

Figure 2 displays the size distributions obtained by spICP-MS. The histograms represent the normalized frequency which is correlated to the Nps concentration in function of the calculated size. It is evident that AuNps' sizes are more uniform compared to AgNps which exhibit a bimodal size distribution. Replicates from the same synthesis show similar histograms indicating consistent size profiles for AuNps across three different syntheses while the size distributions of AgNps vary more from one synthesis to another, particularly for the ratio of the two size populations. This underscores the fact that AuNps synthesis is more repeatable compared to AgNps synthesis[37,38].

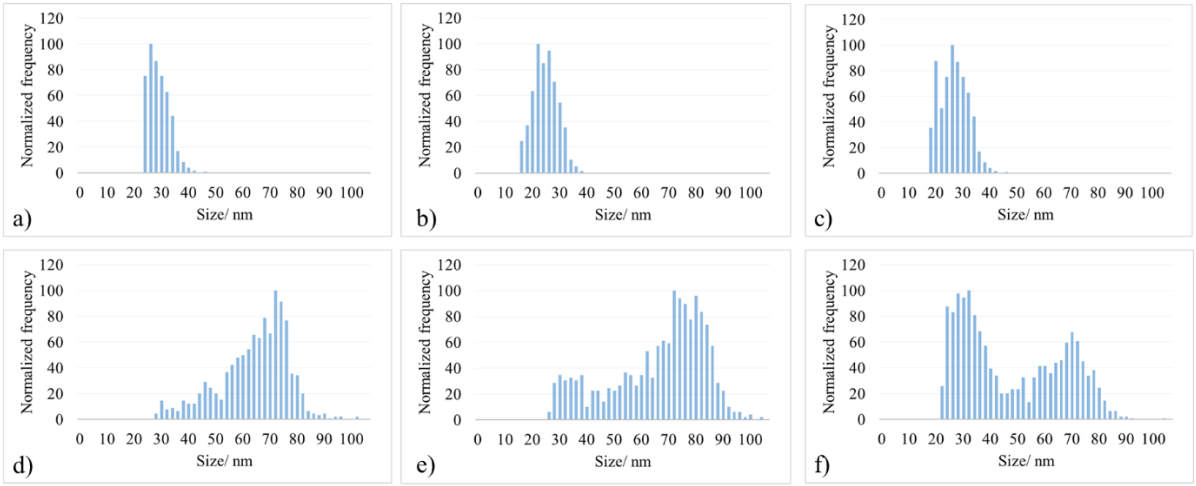

Figure 2. Size dispersion measured by spICP-MS for AuNps (a, b, c for syntheses 1, 2 and 3 respectively) and for AgNps (d, e, f for syntheses 1, 2 and 3 respectively).

3.4 Reference methods for Nps characterization

To confirm spICP-MS results and validate the method, measurements were also performed using techniques commonly used for the SERS substrates characterization which will serve as references[39,40]. Average particle sizes and size distributions were determined by dynamic light scattering (DLS) as well as transmission electron microscopy (TEM). These data combined with the zeta potential are presented in Table 6.

Table 6. Reference techniques results for the characterization of AuNps and AgNps syntheses

	Average size/ nm	Size dispersity (FWHM)	Zeta potential/ mV	TEM estimated size/ nm (n=100)
AuNps S1	38.8	0.53	-43.8	19.8 ± 5
AuNps S2	20.7	0.42	-43.7	-
AuNps S3	17.1	0.36	-42.3	-
AgNps S1	55.6	0.49	-47.1	-
AgNps S2	66.7	0.49	-46.7	62.6 ± 15
AgNps S3	68.2	0.57	-50.6	-

FWHM: full width at half maximum

The characterization data obtained from the reference techniques fall within a similar range although the synthesis variability is more pronounced for AgNps. Since the DLS technique is based on the measurement of hydrodynamic diameter, a smaller size was expected from the spICP-MS measurements. Additionally, the size dispersity considering the full width at half

maximum (FWHM) of the deconvoluted peaks is higher for AgNps than AuNps. For silver, a small fraction of the sample was estimated at approximately 15 nm of average size but was not considered for the measure of peak FWHM. This exclusion leads to an undervaluation of the size dispersion for AgNps. Figure 3 illustrates the deconvolution of distribution peaks for the synthesis 2 of AgNps. For all AgNps syntheses, the fitted peaks match very closely to the measured size distributions ($R^2 > 0.999$ and average percent errors in position of 0.82% maximum).

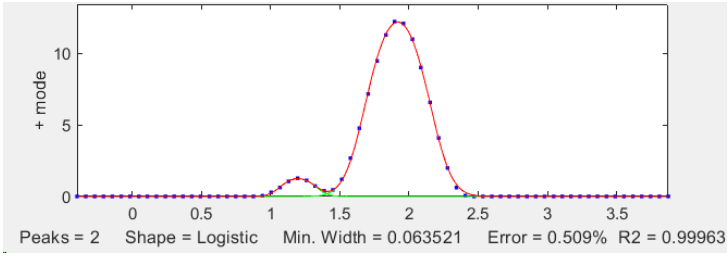

Figure 3. Deconvoluted peaks for the AgNps synthesis 2 considering DLS measurements. The blue dots represent the measured size in log scale, the red line represents the combined model for the two peaks (ideally overlapping the blue dots) and the green lines represents the model components (peakfit.m, version 9.61 and no baseline correction).

Size dispersity can also be observed by TEM, as illustrated in Figure 4. These TEM images confirm the earlier observations, indicating a larger average size and a higher size variability for AgNps. In addition, AgNps exhibit few nanorods in addition to the nanospheres whereas AuNps shapes are notably more uniform.

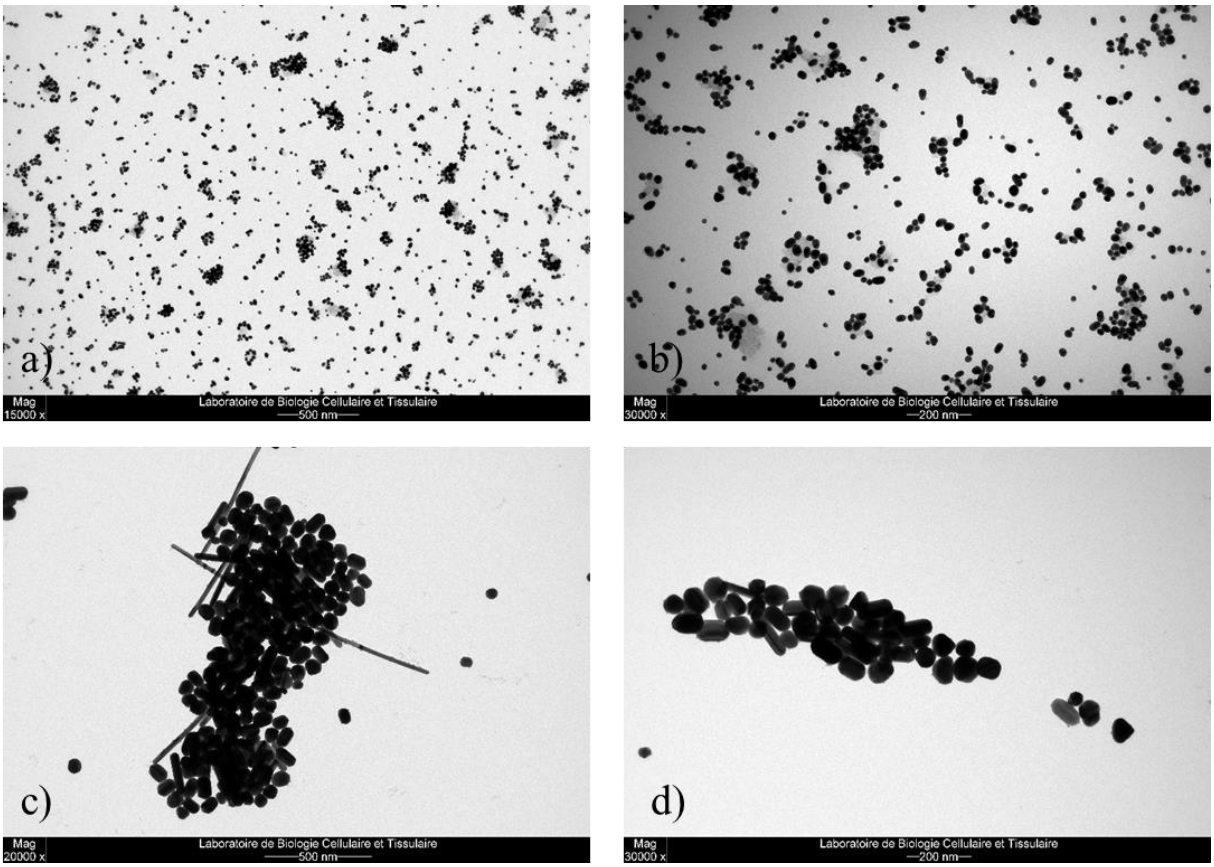

Figure 4. Transmission electron microscopy for AuNps (a: 15 000 magnification, b: 30 000 magnification) or for AgNps (c: 20 000 magnification, d: 30 000 magnification).

Finally, UV-Visible spectroscopy was used to estimate size dispersion and to compare Nps concentration across different syntheses. Figure 5 shows UV-Visible spectra for AuNps and AgNps syntheses. The results align with those obtained from other techniques, reinforcing the observation of higher variability of AgNps' syntheses. Specifically, AuNps spectra for each synthesis show more consistency with one another compared to those of AgNps. The Nps concentrations, indicated by the maximal absorbance, are more homogeneous for AuNps syntheses than for AgNps, as calculated by the spICP-MS. Moreover, the peak width, reflecting the size variability, is notably broader for AgNps indicating less uniformity between syntheses.

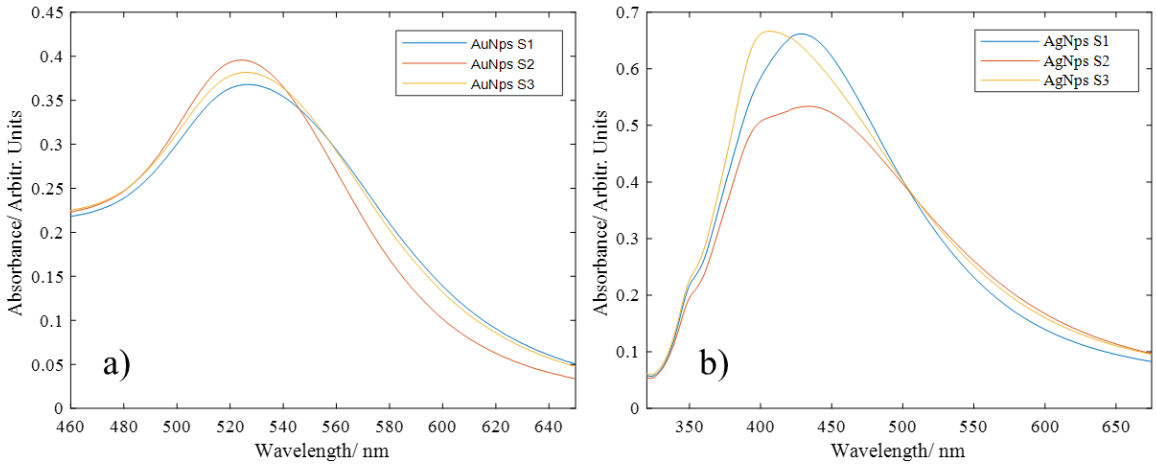

Figure 5. UV-Visible spectra for a) AuNps and b) AgNps.

4. Conclusion

In conclusion, spICP-MS is a powerful tool to characterize SERS substrates made of gold or silver. Indeed, in just one analysis, several information can be obtained namely the mean size, size dispersity and the concentration of Nps. However, this technique assumes a spherical shape of Nps and requires commercial standards for calibration which can be costly. Sample preparation can also be a limiting step as it requires the determination of an appropriate dilution factor for each individual suspension. The obtained results are comparable to those from DLS, TEM or UV-Visible spectroscopy. AuNps and AgNps synthesized by the well-known Lee-Meisel protocol were used to evaluate this method given their widespread use. The comparison of both Nps type confirmed that AuNps have more homogeneous and reproducible properties compared to silver ones. The latter exhibited greater variability in size and shape within the same batch of suspension leading to a significant variability between syntheses which can in turn lead to poor repeatability in SERS intensities.

Although the single particle mode can determine the ionic content, these results are not reliable due to a high dilution of the samples required to ensure that particles reach the plasma individually. Therefore, the conventional ICP-MS mode is more suitable for the determination

of dissolved element concentration. Accordingly, the yield of each reaction was calculated with values close to 100% for both AuNps and AgNps.

Data generated from ICP-MS and spICP-MS analyses could be invaluable to evaluate the synthesis stability over time and to characterize and determine the batch-to-batch repeatability. This information is crucial for the development of reliable SERS substrates for quantitative analyses given that the nature, shape and size of SERS substrates directly impact the signal intensity. In perspectives, methods for the characterization of bimetallic nanoparticles could be developed.

CRediT authorship contribution statement:

Julie Horne: Conceptualization, Methodology, Formal Analysis, Writing - Original Draft Preparation, Writing - Review and Editing. **Pierre Beckers:** Conceptualization, Formal Analysis, Writing – Review and Editing. **Kevser Kemik:** Formal Analysis, Writing – Review and Editing. **Charlotte de Bleye**: Conceptualization, Methodology, Writing - Review and Editing, Supervision. **Pierre-Yves Sacré**: Conceptualization, Writing - Review and Editing. **Nicolas Thelen:** Methodology, Formal Analysis. **Philippe Hubert**: Supervision, Project Administration, Funding Acquisition. **Eric Ziemons**: Conceptualization, Writing - Review and Editing, Supervision, Project Administration. **Cédric Hubert**: Conceptualization, Writing – Review and Editing, Supervision, Project Administration. All authors have read and agreed to the published version of the manuscript.

Acknowledgments: The authors thank Laurence Collard and Géraldine Piel (Laboratory of Pharmaceutical Technology and Biopharmacy, ULiege, Belgium) for the DLS measurements.

Funding: This work was supported by Walloon Region, thanks to a FRIA grant and by the Leon Fredericq foundation.

Conflicts of Interest: The authors declare no conflict of interest. The funders had no role in the study or in the decision to publish the results.

Novelty statement: The inductively coupled plasma mass spectrometry associated to the single particle module was applied for the first time to characterize SERS substrates made of gold and silver.

References:

[1] C. De Bleye, E. Dumont, E. Rozet, P. Y. Sacré, P. F. Chavez, L. Netchacovitch, G. Piel, P. Hubert, E. Ziemons, *Talanta* **2013**, *116*, 899.

[2] R. Goodacre, D. Graham, K. Faulds, *TrAC - Trends Anal. Chem.* **2018**, *102*, 359.

[3] S. Benítez-Martínez, Á. I. López-Lorente, M. Valcárcel, *Microchem. J.* **2015**, *121*, 6.

[4] B. Sharma, M. Fernanda Cardinal, S. L. Kleinman, N. G. Greeneltch, R. R. Frontiera, M. G. Blaber, G. C. Schatz, R. P. Van Duyne, *MRS Bull.* **2013**, *38*, 615.

[5] C. De Bleye, E. Dumont, A. Dispas, C. Hubert, P. Y. Sacré, L. Netchacovitch, B. De Muyt, C. Kevers, J. Dommes, P. Hubert, E. Ziemons, *Talanta* **2016**, *160*, 754.

[6] K. M. M. Abou El-Nour, A. Eftaiha, A. Al-Warthan, R. A. A. Ammar, *Arab. J. Chem.* **2010**, *3*, 135.

[7] I. Hammami, N. M. Alabdallah, A. Al jomaa, M. kamoun, *J. King Saud Univ. - Sci.* , DOI:10.1016/j.jksus.2021.101560.

[8] G. Santos, J. Cuadra, O. Deodanes, C. Violantes, H. Ponce, C. Rudamas, **2021**, *6*, 55.

[9] J. Horne, C. De Bleye, P. Lebrun, K. Kemik, T. Van Laethem, P. Sacr, P. Hubert, E. Ziemons, , DOI:10.1016/j.jpba.2023.115475.

[10] M. M. Modena, B. Rühle, T. P. Burg, S. Wuttke, *Adv. Mater.* **2019**, *31*, 1.

[11] A. Kumar, C. K. Dixit, *Adv. Nanomedicine Deliv. Ther. Nucleic Acids* **2017**, 44.

[12] R. Thomas, *Practical Guide to ICP-MS*, **2008**.

[13] J. Bettmer, M. Montes Bayón, J. Ruiz Encinar, M. L. Fernández Sánchez, M. del R. Fernández de la Campa, A. Sanz Medel, *J. Proteomics* **2009**, *72*, 989.

[14] F. Laborda, E. Bolea, J. Jimenez-Lamana, *Anal. Chem.* **2014**, *86*, 2270.

[15] S. Lee, X. Bi, R. B. Reed, J. F. Ranville, P. Herckes, P. Westerhoff, *Environ. Sci. Technol.* **2014**, *48*, 10291.

[16] M. D. Montaño, B. J. Majestic, Å. K. Jämting, P. Westerhoff, J. F. Ranville, *Anal. Chem.* **2016**, *88*, 4733.

[17] D. Mozhayeva, C. Engelhard, *J. Anal. At. Spectrom.* **2020**, *35*, 1740.

[18] J. Dobias, R. Bernier-Latmani, *Environ. Sci. Technol.* **2013**, *47*, 4140.

[19] J. Tuoriniemi, G. Cornelis, M. Hassellöv, *Anal. Chem.* **2012**, *84*, 3965.

[20] H. E. Pace, N. J. Rogers, C. Jarolimek, V. A. Coleman, C. P. Higgins, J. F. Ranville, *Anal. Chem.* **2012**, *84*, 4633.

[21] A. Hineman, C. Stephan, *J. Anal. At. Spectrom.* **2014**, *29*, 1252.

[22] A. R. M. Bustos, M. R. Winchester, *Anal. Bioanal. Chem.* **2016**, *408*, 5051.

[23] H. Goenaga-Infante, D. Bartczak, *Charact. Nanoparticles Meas. Process. Nanoparticles* **2019**, 65.

[24] J. Liu, K. E. Murphy, R. I. Maccuspie, M. R. Winchester, *Anal. Chem.* **2014**, *86*, 3405.

[25] F. Laborda, J. Jiménez-Lamana, E. Bolea, J. R. Castillo, *J. Anal. At. Spectrom.* **2011**, *26*, 1362.

[26] I. Abad-Álvaro, E. Peña-Vázquez, E. Bolea, P. Bermejo-Barrera, J. R. Castillo, F. Laborda, *Anal. Bioanal. Chem.* **2016**, *408*, 5089.

[27] A. C. Gimenez-Ingalaturre, K. Ben-Jeddou, J. Perez-Arantegui, M. S. Jimenez, E. Bolea, F. Laborda, *Anal. Bioanal. Chem.* **2023**, *415*, 2101.

[28] G. Cornelis, M. Hassellöv, *J. Anal. At. Spectrom.* **2014**, *29*, 134.

[29] W. W. Lee, W. T. Chan, *J. Anal. At. Spectrom.* **2015**, *30*, 1245.

[30] J. Liu, K. E. Murphy, M. R. Winchester, V. A. Hackley, *Anal. Bioanal. Chem.* **2017**, *409*, 6027.

[31] P. C. Lee, D. Meisel, *J. Phys. Chem.* **1982**, *86*, 3391.

[32] *Eur. Pharmacop.*, **2008**, 118–119.

[33] IPF, https://terpconnect.umd.edu/~toh/spectrum/InteractivePeakFitter.htm#Keypress_operated_version:_ipf.m, (accessed 2 February 2024).

[34] L. V. Rajaković, D. D. Marković, V. N. Rajaković-Ognjanović, D. Z. Antanasijević, *Talanta* **2012**, *102*, 79.

[35] J. Vidmar, R. Mila, A. Mladenovi, J. Šč, **2018**, *634*, 1259.

[36] J. B. Deshpande, S. Chakrabarty, A. A. Kulkarni, *Chem. Eng. J.* **2021**, *421*, 127753.

[37] J. F. Betz, W. W. Yu, Y. Cheng, I. M. White, G. W. Rubloff, *Phys. Chem. Chem. Phys.* **2014**, *16*, 2224.

[38] E. Dumont, C. De Bleye, J. Cailletaud, P. Y. Sacré, P. B. Van Lerberghe, B. Rogister, G. A. Rance, J. W. Aylott, P. Hubert, E. Ziemons, *Talanta* **2018**, *186*, 8.

[39] E. Dumont, C. De Bleye, M. Haouchine, L. Coïc, P. Y. Sacré, P. Hubert, E. Ziemons, *Spectrochim. Acta - Part A Mol. Biomol. Spectrosc.* **2020**, *233*, 118180.

[40] J. Cailletaud, C. De Bleye, E. Dumont, P. Y. Sacré, Y. Gut, L. Bultel, Y. M. Ginot, P. Hubert, E. Ziemons, *Talanta* **2018**, *188*, 584.